atmosphere

MDPI

Article

Sensitivity Analysis of Pipe–Soil Interaction Influencing Factors under Frost Heaving

Long Huang [1,*], Yu Sheng [2], Liping Chen [1], Erxing Peng [2], Xubin Huang [3] and Xiyan Zhang [2]

[1] School of Civil Engineering, Lanzhou Institute of Technology, Lanzhou 730050, China
[2] State Key Laboratory of Frozen Soil Engineering, Northwest Institute of Eco-Environment and Resources, Chinese Academy of Sciences, Lanzhou 730000, China
[3] Northwest Engineering Corporation Limited, Power China, Xi'an 710065, China
* Correspondence: huanglong@lzb.ac.cn; Tel.: +86-181-8953-8646

Abstract: The mechanism of pipe–soil interaction under frost heaving is complicated due to many factors affecting the pipe–soil system. In order to analyze the sensitivity of various pipe–soil interaction influencing factors and highlight the relationship between the factors and the pipe's mechanical characteristics during frost heaving, a pipe–soil interaction model based on a semi-infinite elastic frozen soil foundation is developed. Besides, the mechanical indices characterizing the influence factors and their change law are emphatically explored. The results show that the pipe stress changes most obviously at the transition region between the frost-heaving and non-frost-heaving regions. The equivalent stress increases nonlinearly with the increase of foundation coefficient, linearly with the increase of frost heave and elastic modulus of pipe, and decreases nonlinearly with the increase of transition length and pipe wall thickness. The peak stress of the pipe increases linearly with the increase of temperature difference. Moreover, the maximum allowable frost heave deformation decreases nonlinearly with the increase of oil pressure. This study helps provide theoretical reference for the adjustment, control, and prediction of stress and deformation in the design of buried pipelines under frost heaving.

Keywords: buried pipe; soil; frost heave; interaction; influencing factors; sensitivity

Citation: Huang, L.; Sheng, Y.; Chen, L.; Peng, E.; Huang, X.; Zhang, X. Sensitivity Analysis of Pipe–Soil Interaction Influencing Factors under Frost Heaving. *Atmosphere* **2023**, *14*, 469. https://doi.org/10.3390/atmos14030469

Academic Editor: Lin Chen

Received: 26 December 2022
Revised: 22 February 2023
Accepted: 23 February 2023
Published: 27 February 2023

1. Introduction

Pipe–soil interaction caused by freezing and thawing has always been a hot research topic, where frost heaving is a serious problem that has been challenging engineers for a long time [1]. When the buried oil and gas pipeline crosses a frost-heaving area, the differential frost heave of soil at the pipe bottom causes obvious deformation and stress concentration between the frost-heaving and non-frost-heaving regions along the pipeline, which results in a significantly increased pipe internal bending moment and shear force that threaten the overall safety of the pipeline [2,3]. Serious accidents such as pipeline rupture and perforation, oil leakage and pollution, and fire and explosion significantly impact the local environment, climate, and surface energy balance [4–6]. For pipe design in engineering practice, the critical problem is how significant and what form of frost heaving forces the pipe operational failure, what external and internal factors have a significant influence on the stress of the pipe–soil system, and how to reduce or eliminate the potential damage of frost heaving to the pipe [7,8]. Therefore, analyzing the sensitivity of influencing factors on the interaction between buried pipe and foundation soil under frost heaving is essential for the structural design, disease prevention, and safe operation of pipelines in cold regions.

The pipe–soil interaction under frost heaving is a dynamic equilibrium process. The dynamic stability of the pipe–soil system depends on the pipe's physical properties, the soil's characteristics, environmental factors, engineering conditions, and the pipe's fluid properties [9]. However, it is important to establish a reasonable model of pipe–soil interaction. Previously, scholars have conducted a series of investigations, monitoring, surveying, experiment, simulation, and calculation work for the pipeline; the elastic foundation beam based on Winkler's elastic theory is also the most widely used simplified model for studying pipelines [10–18]. Besides, some scholars developed computer programs based on the finite element method to analyze the effects of the pipe joint, bedding heterogeneities, soft soil, high temperature, and frost heaving on the long-distance pipeline's deformation and stress distribution law [19–25]. In the early 21st century, some scholars considered the nonlinear problem (involving fault, landslide, earthquake, thawing, etc.) between the pipe and soil to investigate the effects of various soil and pipeline parameters on pipe structural response, identify pipeline failure, simulate the interaction between buried pipe and surrounding soil by finite element method, and analyze parameters affecting the mechanical properties of buried pipe [26–32]. In addition, some researchers have analyzed the sensitivity and stability of submarine pipe–soil interaction and studied the influence of different key parameters on the dynamic response and fatigue life of the pipe under complex and influential factors, including bending, axial force, external hydrostatic pressure, ocean waves and currents, surrounding soils, seabed flexibility, and burial depth [33–36]. Based on the actual situation of oil pipelines in cold regions, the frost heave of surrounding soil varies significantly with the soil type and the humidity and thermal conditions of the ground. It can lead to large upward movements of a pipeline and is caused by the interaction between the longitudinal compressive force present during operation and overbend irregularities in the profile [37]. On the other hand, the interaction between pipe and soil is a complex problem that includes nonlinearity, elastoplasticity, viscoplasticity, dilatancy, and anisotropy [38–40]. Some researchers considered the effects of frost heaving, oil pressure, and thermal stress to analyze the distribution law of axial tensile strain of pipe under different lengths, wall thickness, and oil pressure and put forward the design criteria based on axial strain; some presented additional calculations to explore the influence of pipeline temperature, pipe insulation, and ground temperature on frost heave of buried pipelines [41–44]. Moreover, a stress analysis of municipal buried water pipes during the cold wave period takes into account the factors influencing the pipe's stresses and considers the impact of air temperature and the relationship between the pipe's buried depth and the soil's freezing depth [45].

The above pipeline research achieved good results and provided important theoretical support to promote deep learning for pipe–soil interaction in the frozen soil environment. There are few studies on the laws of various indicators in the process of pipe–soil interaction under frost heaving conditions, and no universal model can be applied to the pipe–soil interaction. For practical engineering applications, the most suitable method is to select a simplified model that can consider the main factors affecting the stress–strain relationship and then analyze the impact of other factors on critical indicators in the pipe–soil model. This paper uses the elastic foundation beam theory to develop a buried pipe model under frost heaving [13,41,43]. The purpose herein is to analyze the sensitivity of relevant influencing factors in the process of pipe–soil interaction; that is, to quantitatively analyze the influence on parameter changes to the key indices (stress and strain) in the pipe–soil system. The effects of factors such as temperature difference, oil pressure, earth pressure, foundation coefficient, pipe size, and elastic modulus are reflected as the pipe's stress or strain to reveal the influence of various indices on the stress distribution at the pipe top when it is subjected to frost heaving.

2. Equivalent Stress and Principal Stresses

2.1. Equivalent Stress

This study defines the yield criterion in the fourth strength theory as the equivalent stress σ_e (Von Mises stress σ_v) to comprehensively measure pipe stress under the combination of the principal stresses (σ_1, σ_2, and σ_3) [46,47]. The equivalent stress is calculated as follows:

$$\begin{aligned}\sigma_e = \sigma_v &= \sqrt{\frac{1}{2}\left[(\sigma_1-\sigma_2)^2+(\sigma_2-\sigma_3)^2+(\sigma_3-\sigma_1)^2\right]} \\ &= \sqrt{\frac{1}{2}\left[(\sigma_c-\sigma_a)^2+(\sigma_a-\sigma_r)^2+(\sigma_r-\sigma_c)^2\right]}\end{aligned} \tag{1}$$

After superposition, all stresses on the pipe are transformed into spatial circumferential (σ_c), axial (σ_a), and radial (σ_r) stresses. The axial stress is mainly determined by the frost heaving and temperature stress-induced pipe bending, while the circumferential stress and radial stress are mainly determined by oil pressure, temperature difference, frost-heaving force, and soil pressure.

2.2. Pipe Stresses Caused by Frost Heaving

The frost heave that may exist in linear engineering (such as railways, highways, oil and gas pipelines, channels, and culverts) has a gradual process. When a pipeline crosses from a frost-heaving region to a non-frost-heaving region, a frost-susceptible soil to a non-frost-susceptible soil, or from frozen soil to an unfrozen one, the pipeline is subjected to differential movements caused by differential frost heave at the interface of the two regions [41,48]. According to the basic principle of mechanics, there is a stress mutation at the interface, which produces maximum bending moment under the most unfavorable conditions [49,50]. In order to realistically analyze a pipe while reflecting its stress distribution, a transition region and interface are typically assumed to calculate the stress peak under mutation and then preliminarily design the pipe through the stress peak. The frost heave of soil at the pipe bottom is represented as shown in Figure 1.

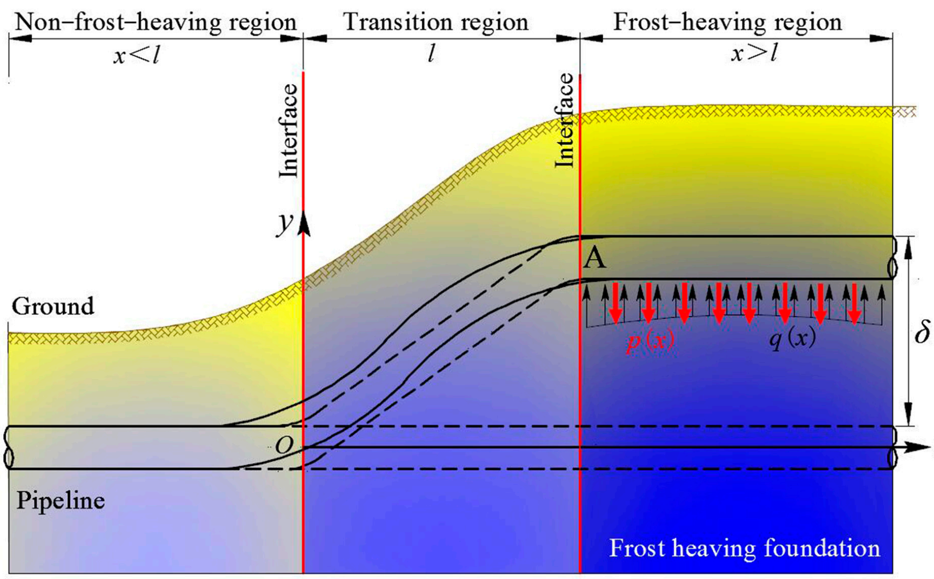

Figure 1. The stress diagram of pipe under frost heaving.

When assuming a full pipe–soil contact with no slippage between the pipe and the foundation soil, the soil does not crumble with the pipe moving up under frost heaving. The primary differential elastic foundation beam equation, while ignoring the lateral displacement, can be written as follows [51–53]:

$$E_P I_P \frac{d^4\omega(x)}{dx^4} + p(x) = q(x) \tag{2}$$

where $p(x) = k\omega(x)$ is the contact pressure (foundation reaction), k is the foundation coefficient of frozen soil, $q(x) = p_t(x) + p_z(x) - p_d(x)$ is the total load at the pipe bottom,

$p_t(x)$, $p_z(x)$, and $p_d(x)$ are the soil pressure, the pipe weight, and the frost-heaving force, respectively, $\omega(x)$ is the foundation displacement, and $E_P I_P$ is the pipe stiffness.

For the convenience of obtaining the analytical solution of Equation (2), this study assumes that the frost heave increases linearly from a non-frost-heaving region to a frost-heaving region, and the frost-heaving amount (or longitudinal uplift deformation of the pipeline) is expressed as follows:

$$\omega(x) = \begin{cases} \delta, x > l \\ \frac{\delta}{l}x, 0 < x < l \\ 0, x < l \end{cases} \tag{3}$$

The general solution of the elastic foundation beam equation [46,54] when $x > l$, i.e., $\omega(x > l) = \delta$ is shown in Equation (4), when $0 < x < l$, i.e., $\omega(0 < x < l) = \frac{\delta}{l}x$ is shown in Equation (5), and when, $x < 0$, i.e., $\omega(x < 0) = 0$, is shown in Equation (6).

$$\omega_1 = e^{\beta x}[A_1\cos(\beta x) + B_1\sin(\beta x)] + e^{-\beta x}[C_1\cos(\beta x) + D_1\sin(\beta x)] + \delta \tag{4}$$

$$\omega_2 = e^{\beta x}[A_2\cos(\beta x) + B_2\sin(\beta x)] + e^{-\beta x}[C_2\cos(\beta x) + D_2\sin(\beta x)] + \frac{\delta}{l}x \tag{5}$$

$$\omega_3 = e^{\beta x}[A_3\cos(\beta x) + B_3\sin(\beta x)] + e^{-\beta x}[C_3\cos(\beta x) + D_3\sin(\beta x)] \tag{6}$$

where β is the characteristic coefficient related to the pipeline's elastic properties and the frozen soil foundation $\beta = \sqrt[4]{\frac{4EI}{k}}$.

In this study, the boundary conditions to be satisfied include $\omega = \delta$ at $x \to \infty$ and $\omega = 0$ at $x \to -\infty$. Besides, multiple continuity conditions were assumed at O ($x = 0$) and A ($x = l$). Indeed, the piecewise equations and the first, second, and third equations' derivatives on both sides of the interface were equalized to obtain a set of eight equations that determine the deflection curves. Thereafter, the bending equation of the pipeline and the relationship between the shear force Q, the bending moment M, and the load concentration $q(x)$ were utilized to derive the rotation angle, bending moment, shear force, and load.

Moreover, the soil pressure on any side around the pipe was assumed to be uniformly loaded with a lateral and vertical frost heaving pressure concentration, and the distributions of stress and strain on the cross-section of the circular pipe embedded in the medium were elastically analyzed as a stress concentration problem of the hole. Once the pressure was superimposed on the surrounding boundaries, the stress component of any point was obtained using the elastic theory [47,55].

2.3. Temperature Stress and Oil Pressure

The temperature difference inside and outside the pipe has a major influence on the temperature field along the pipeline, then affects the stress–strain state of the pipe–soil interaction during frost heaving [56–58]. In this study, the solution to the temperature stress of the pipe–soil system was simplified as a boundary problem in the temperature field, and the boundary conditions were formulated according to the law of heat exchange between the object surface and the surrounding medium. Therefore, this study assumes that the temperature at the pipe's inner wall ($r = r_0$) increases to T_r, and the temperature at the pipe's outer wall ($r = R_0$) increases to T_R. Theoretically, based on the differential equation ($\frac{\partial T}{\partial t} - \alpha\nabla^2 T = \frac{\partial\theta}{\partial t} = \frac{W}{cr}$) of heat conduction, the pipe–soil system's temperature field tends to be stable when the heat flow remains stable ($\frac{\partial T}{\partial t} = 0$) at zero heat source in the pipe ($\frac{\partial\theta}{\partial t} = 0$). The variation law of temperature satisfies the differential equation $\nabla^2 T = 0$, that is, $\left(\frac{d^2}{dr^2} + \frac{1}{r}\frac{d}{dr}\right)T = 0$. Assuming that the buried pipeline is a finite-length thin-walled element with unconstrained ends, the expression of the thermal stress state at a certain point of the pipe can be obtained from the thermoelastic theory of thin-walled pipes [42,52,55].

Oil pressure is one of the main factors affecting pipe strength [59]. Generally, the thickness of the pipe wall can be determined according to the design's oil pressure to obtain the pipe materials' consumption. The calculation of oil pressure is necessary to ensure the pipeline's reliability. However, only considering oil pressure cannot ensure the strength and stability of the pipeline when other influencing factors coexist. Accordingly, this study assumes the pipeline to be buried in an infinite elastic soil with frost heaving. The cross-sectional stress of the pipe caused by oil pressure was simplified as the uniformly distributed pressure (uniform stress field) on the inner wall of a cylinder, and the stress and strain of the pipe–soil system are calculated as an axisymmetric system. The pipe and frozen soil have different elastic moduli, assuming they are in full contact and without mutual sliding. The pipe–soil system maintains dynamic equilibrium, with boundary and equilibrium conditions on the interface between the two. Thus, the normal stress, the shear stress, the normal displacement, and the tangential displacement on the soil and pipe surface are equal, respectively. Considering the frost heaving effect, the frost-heaving force of frozen soil around the pipe was simplified as a uniformly distributed load along the pipe's outer wall. According to the boundary conditions of the uniform stress field inside and outside the thin-walled pipe, the three-dimensional stresses at a point on the pipe wall were obtained from the Lame stress solution under axisymmetric stress and displacement [41,52,55].

2.4. Overlying Soil Pressure

Currently, most calculation methods regarding the soil pressure are improved based on the Marston–Spangler theory, which assumes that the overlying soil of the buried pipeline is a soil column with a sliding surface formed by the deformation between the pipeline and the foundation. Considering the influence of the foundation and the relative stiffness of pipe and soil and taking any micro-element within the sliding surface for analysis, the calculation formula of the overlying soil pressure was derived based on the stress balance condition ($\sum F_\theta = 0$) as follows [60]:

$$\sigma_v^s = \eta f \left[R_0 \gamma H + \frac{\gamma \left(2HH_e - {H_e}^2 \right) (\tan\theta - \tan\varphi)}{\tan^2\theta} \right] \tag{7}$$

where H is the buried depth of pipeline (m), H_e is the height of equal settlement plane (m), γ is the unit weight of soil (kg/m^3), φ is the internal friction angle of overlying soil (rad), f is the influence coefficient of the relative stiffness of pipe and soil, η is the influence coefficient of the foundation form, and θ is the angle between the sliding surface and the horizontal plane (rad) given as $\theta = \frac{\pi}{4} + \frac{\varphi}{15}\left(\frac{H}{R_0}\right)$.

2.5. Weight of Pipe and Medium

Indeed, the weight of the pipe and medium are far less than the frost-heaving force in practice. Therefore, its influence can be ignored during the stress calculation. On the other hand, when considering the impact of pipe material characteristics, the pipe weight q_p^w(N), gas weight q_g^w(N), and oil weight q_o^w(N) can be calculated according to the following formula [61]:

$$\begin{cases} q_p^w = \pi(R_0 - \delta_P) L \delta_P \rho_p g \\ q_g^w = 100 P_s {r_0}^2 L g \\ q_o^w = \rho_y L \frac{\pi {r_0}^2}{4} g \end{cases} \tag{8}$$

where P_s is the standard pressure (MPa), L is the calculated pipeline length (m), δ_P is the pipe's wall thickness, ρ_p is the pipe material density, ρ_y is the crude oil unit weight and g is the gravitational acceleration ($g = 9.8$ N/kg).

3. Sensitive Analysis of Influencing Factors on Pipe–Soil Interaction

3.1. Foundation Coefficient

3.1.1. Elastic Modulus

The elastic modulus of frozen soil mainly depends on the particle composition, soil temperature, water content, and external pressure, in which the temperature is the dominant factor. A test shows that the elastic modulus of soft soil in a specific area varies nonlinearly with temperature [62,63]:

$$E_s = \alpha T^n + \beta \tag{9}$$

where α, β, and n are the test coefficients.

The elastic modulus is often measured through infinite, triaxial, and consolidation compression tests. In order to facilitate estimation, a weighted average of the elastic modulus of multiple single soil layers on the thickness can be utilized to calculate the elastic modulus of the thicker foundation [64]. Within a specific temperature range, the change of the average elastic modulus of single-layer frozen soil with negative temperature can be fitted approximately by a linear equation.

3.1.2. Poisson's Ratio

Although the idealized soil cannot fully reveal the inherent properties of frozen soil, it still requires idealizing the frozen soil and simplifying the analysis process in practical problems. The elastic modulus and the Poisson's ratio can be used as parameters to characterize the mechanical characteristics of the idealized frozen soil. Yao [65] determined the relationship between the Poisson's ratio and temperature for frozen silty clay when the water content is 18%, 25%, and 30%. The results indicate that the Poisson's ratio grows with the temperature and water content. Therefore, to match the parameters of the previous pipeline frost heaving test [48], the linear relationship between the Poisson's ratio and temperature at the water content of 30% was obtained by fitting Yao's test data, which can be expressed as Equation (10). Moreover, this relationship is one of the preconditions for the selection of subsequent calculation parameters in this paper.

$$\begin{cases} \mu_s = 0.015T + 0.2904 \\ R^2 = 0.9846 \end{cases} \tag{10}$$

3.1.3. The Coefficient of Frozen Soil Foundation

The coefficient of the frozen soil foundation at the pipeline's location represents the deformation capacity of frozen soil. It can be expressed under specific conditions by the elastic modulus, the Poisson's ratio, and other constant parameters of the frozen soil. Based on the elastic theory, empirical formula, and elastic modulus conversion formula under the triaxial load test, the elastic semi-infinite foundation model, consolidation test value, and the foundation coefficient formula were derived by Vlazov, Biot, Vesic, Scheidig, Woinowsky, and others [66,67]. Figure 2 indicates that the foundation coefficient variation with temperature is based on the foundation coefficient formula [47].

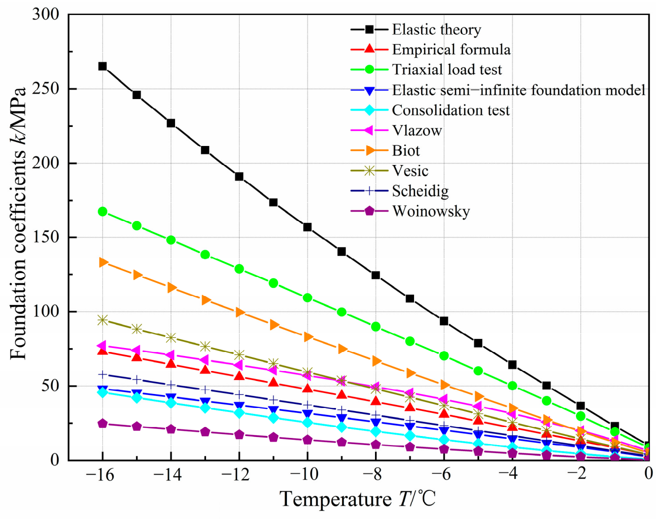

Figure 2. The relationship between foundation coefficient and temperature of different empirical formulas.

According to the relationship between the above parameters and the actual situation of the China–Russia crude oil pipeline [68], the following control parameters are chosen: w_0 = 30%, T_r = 10 °C, T_R = −3 °C, E_s = 26.2 MPa, δ= 0.4 m. The empirical formulas of the elasticity theory, triaxial load test, Vlazov and Scheidig were selected for analysis, and the empirical values of the foundation coefficient based on the above control parameters were converted as shown in Table 1. Then, the equivalent stress distribution of the pipe was calculated based on various foundation coefficients, as depicted in Figure 3.

Table 1. The values of the foundation coefficient from different empirical formulas.

Grade	Elastic Theory	Triaxial Load Test	Vlazov	Scheidig
Formula k	$\frac{E_s}{R(1+\mu_s)}$	$\frac{1.2E_s}{B(1-\mu_s{}^2)}$	$\frac{E_s}{H(1+\mu_s)(1-2\mu_s)}$	$\frac{2E_s}{B\log\left(1+2\frac{H}{B}\right)}$
Value	50.2	39.9	25.8	13.0

Note: B is the calculated pipeline width, and H is the buried pipeline depth.

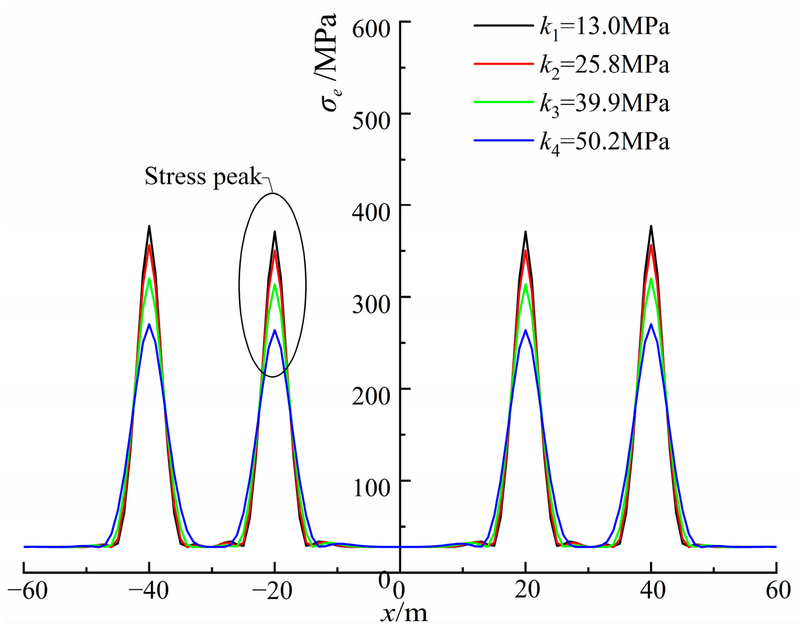

Figure 3. The equivalent stress of pipe under different foundation coefficients.

Figure 3 reveals that the pipe stress varies most obviously at the transition region between the non-frost-heaving and the frost-heaving regions, where there is a stress peak at the interface. Figure 4 illustrates the relationship between the equivalent stress and the foundation coefficient using the maximum value of equivalent stress at the interface under the various foundation coefficients as the analysis target. It shows that the equivalent stress increases nonlinearly as the foundation coefficient rises. Considering varied oil pressure conditions and pipe wall thickness, the higher the oil pressure in the pipe, the thinner the pipe wall thickness, and the greater the equivalent stress. Under the same oil pressure (7 MPa), the foundation coefficient increases from 13 MPa to 50.2 MPa, the equivalent stress grows from 270.5 MPa to 377.7 MPa, and the equivalent stress rises by 39.6% when the foundation coefficient increases by 286% (Figure 4a). The equivalent stress develops from 315 MPa to 434.3 MPa, and the equivalent stress rises by 37.9% using the same wall thickness (10 mm) (Figure 4b). In other words, the foundation coefficient grows by 286%, and the equivalent stress increases by about 38.5%, while all other contributing elements remain unchanged.

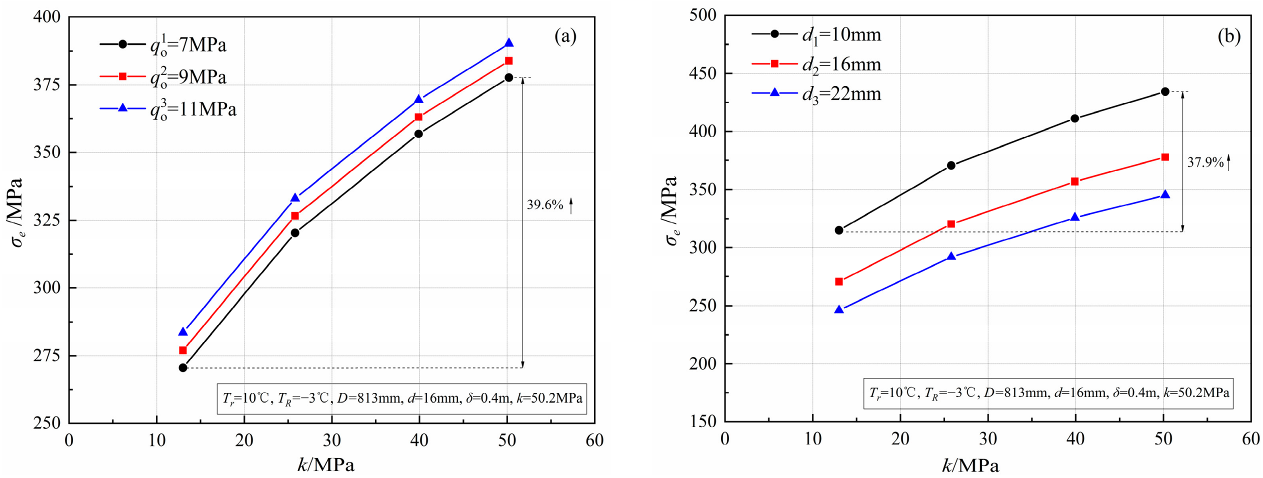

Figure 4. Variations in the equivalent stress with respect to the foundation coefficient. (**a**) Under different oil pressures; (**b**) Under different wall thicknesses.

3.2. Temperature Difference

Referring to the actual situation of the China–Russia oil pipeline, the difference in temperature between the inside and the outside of the pipeline was examined in the range of −25 °C to 10 °C. The maximum differential frost heave was assumed $\delta = 0.4$ m, the elastic modulus of frozen soil $E_s = 26.2$ MPa, the Poisson's ratio $\mu_s = 0.2454$, and the foundation coefficient $k = 50.2$ MPa. Regardless of the impact of other factors, Figure 5 represents the influence of temperature difference on the stress peak of the pipe based on the most unfavorable temperature difference situation. Figure 5 indicates that the peak stress increases linearly when the temperature difference rises from 10 °C to 20 °C with the same wall thickness (10 mm), the equivalent stress increases from 430.7 MPa to 443.1 MPa, and the equivalent stress grows by 2.9% when the temperature difference increases by 100%. Considering the pipe wall thickness condition, it is evident that raising the wall thickness can reduce the peak stress of the pipe. Therefore, in engineering practice, increasing the pipe thickness can minimize pipe deformation and make the pipe more resistant to frost heaving.

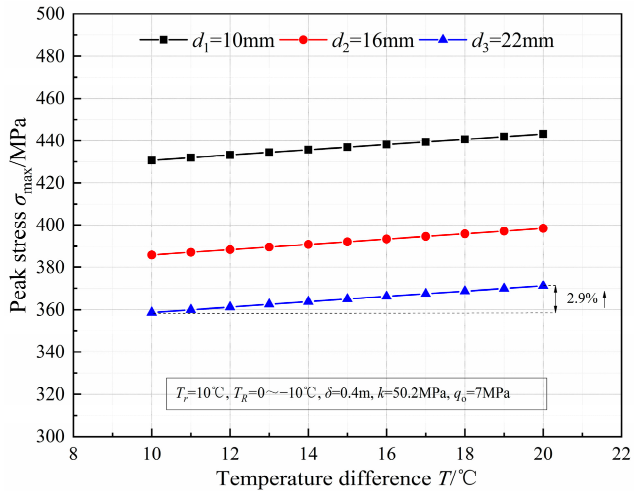

Figure 5. Pipe stress peak caused by temperature differences under various pipe wall thicknesses.

3.3. Frost Heave

Assuming that the pipe is in complete contact with the frozen soil foundation, the frost heave at the pipe bottom is consistent with the pipe's deflection. The foundation coefficient measures the deformation strength of the soil, whereas frost heave determines the soil's deformation. The pipe stress distribution was calculated under the condition of various frost heaves ($\delta_1 = 0.2$, $\delta_2 = 0.4$, $\delta_3 = 0.6$, and $\delta_4 = 0.8$), and the change of the maximum equivalent stress at the interface was observed by considering the effect of temperature difference, soil pressure, and oil pressure. The computed equivalent stress value exhibits a linear increase with frost heave change (Figure 6). Under the same oil pressure (7 MPa), the amount of frost heaving increases from 0.2 m to 0.8 m, the equivalent stress grows from 191.9 MPa to 750.6 MPa, and the equivalent stress develops by 291% (Figure 6a). The equivalent stress rises from 227.5 MPa to 851.3 MPa, and the equivalent stress grows by 274% under the same wall thickness (10 mm) (Figure 6b). Considering different oil pressure and pipe wall thickness, the impact of oil pressure on the equivalent stress is not negligible, but the effect of material size (pipe wall thickness) is relatively significant. Therefore, as the frost heave continues to develop, the oil pressure can be regarded as a secondary factor, and the material size is the main factor affecting the pipe stress, demonstrating once again that the equivalent stress of the pipe can be lowered by altering the pipe wall thickness.

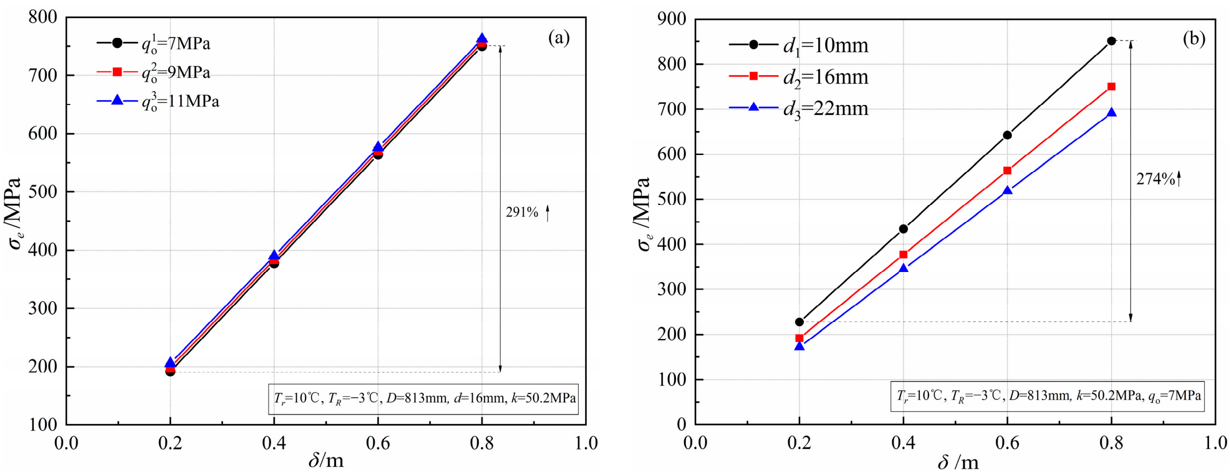

Figure 6. Variations of equivalent stresses with frost heave. (**a**) Under different oil pressures; (**b**) Under different wall thicknesses.

3.4. Oil Pressure in the Pipe

The calculation and analysis parameters were selected by ignoring the effect of thermal expansion and cold contraction of pipes and temperature loss along the pipeline ($T_r = 10$ °C, $T_R = -3$ °C, $E_s = 26.2$ MPa, $\mu_s = 0.2454$, and $k = 50.2$ MPa). Since the internal oil pressure does not affect the axial stress of the pipe, the maximum allowable frost heave deformation of the pipe under the oil pressure condition was calculated (Figure 7). Figure 7 reveals that the maximum allowable frost heave deformation decreases rapidly as the oil pressure increases. According to the comprehensive influence of pipe wall thickness ($d_1 = 10$ mm, $d_2 = 16$ mm, and $d_3 = 22$ mm) and oil pressure, it was found that the smaller the wall thickness, the higher the oil pressure, and the faster the maximum allowable frost heave deformation decreases.

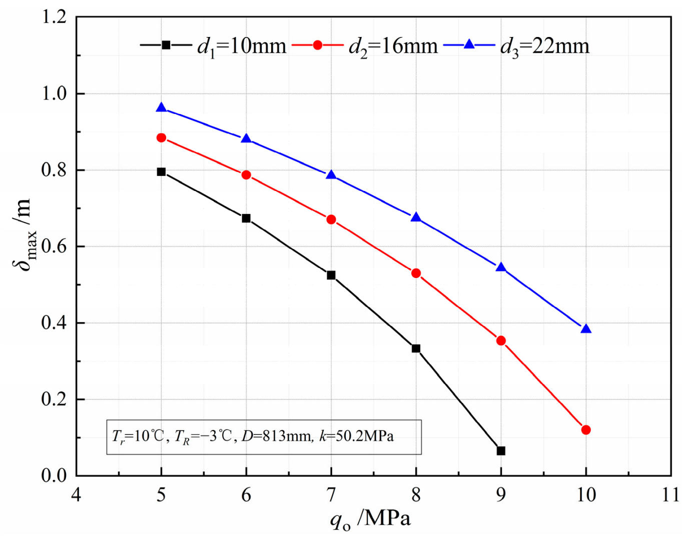

Figure 7. Effect of oil pressure on maximum allowable frost heave deformation.

3.5. Length of the Transition Region (Frost Heaving Range)

Keeping all other parameters constant and assuming that the frost heave reaches 0.4 m, Figure 8 illustrates the deflection curve of the pipeline under the conditions of different transition regions ($l_1 = 5$ m, $l_2 = 10$ m, $l_3 = 20$ m, and $l_4 = 40$ m) according to the elastic foundation beam model under the condition of frost heaving.

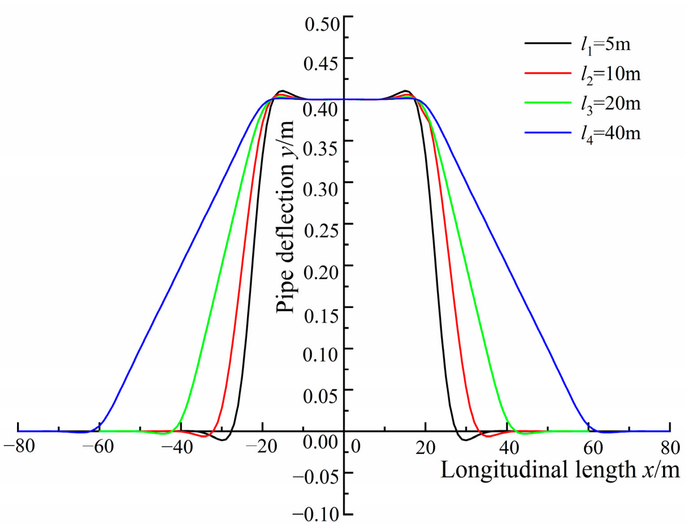

Figure 8. Deflection of pipe under different lengths of the transition region.

Additionally, the duration of the transition region determines the flatness or steepness of the pipeline deformation during the transition from the frost-heaving region to the non-frost-heaving one and impacts the peak stress at the pipeline interface. The shorter the distance of the transition area, the larger the deformation and the stress peak at the interface, making the stress concentration phenomenon more likely. The longer the transition region, the smoother the displacement curve at the interface of the transition region, and the lower the peak stress. Under certain regional conditions, the larger the frost heaving range, the shorter the transition region, and vice versa.

Figure 9 indicates the effect of the transition region length on the equivalent stress. It can be observed that the equivalent stress value drops as the length of the transition region increases. When the transition region expands from 5 m to 40 m, the equivalent stress first decreases rapidly and then decreases slowly. The equivalent stress shows a nonlinear decreasing trend with the length of the transition region, with a large decreasing rate from 5 m to 20 m and a low decreasing rate from 20 m to 40 m, indicating that the greater the frost heaving range, the more uniform the lifting effect on the pipeline and the smaller the impact on the pipe stress. For the influencing factors such as oil pressure, foundation coefficient, temperature difference, and frost heave, the frost heave has the greatest effect on the equivalent stress, whereas the oil pressure has the least influence. Figure 10 shows the impact of the transition region length on the maximum allowable frost heave deformation. The maximum allowable frost heave deformation increases significantly with the length of the transition region, indicating that the longer the transition region, the greater the effect of improving the allowable frost heave deformation. Increasing the length of the transition region is not necessarily significant if the equivalent stress must be reduced to maintain a certain allowable deformation. However, it can slow the growth of equivalent stress, indicating that the selection of transition length significantly impacts the pipe stress in the design or stress calculation of the pipeline when frost heaving occurs.

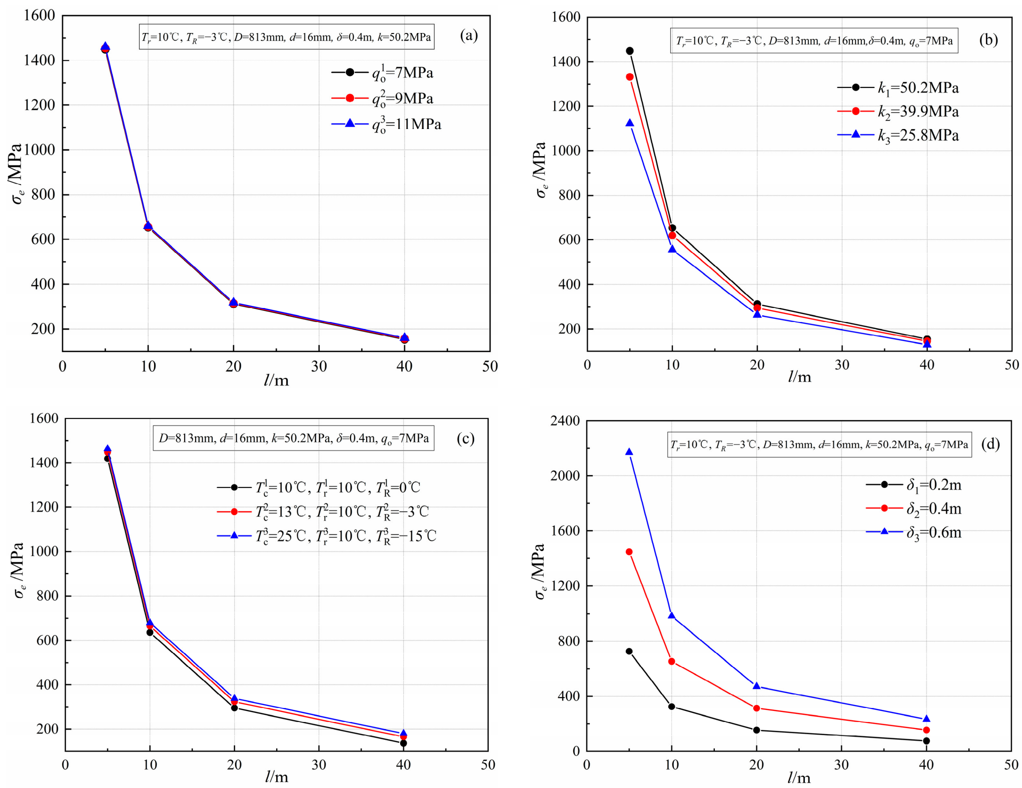

Figure 9. Variations in the equivalent stresses with the length of the transition region. (**a**) Under different oil pressures; (**b**) Under different foundation coefficients; (**c**) Under different temperature differences; (**d**) Under different frost heaves.

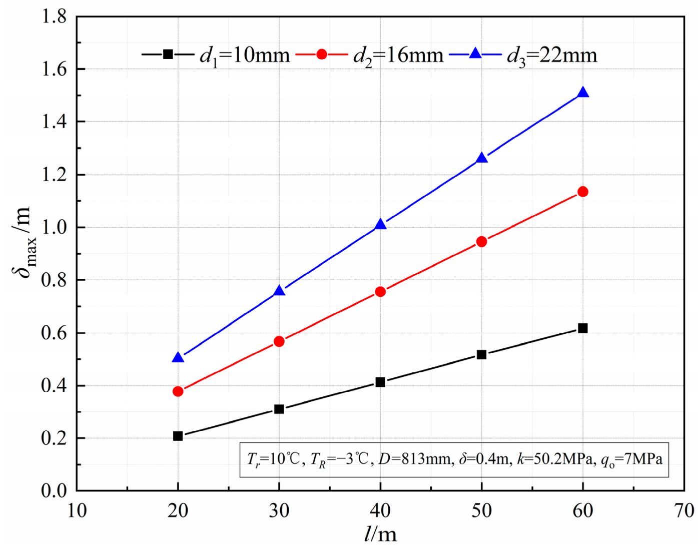

Figure 10. Effect of transition length on maximum allowable frost heave deformation.

3.6. Pipe Size

Analyzing and comparing the following conditions: the same frost heave ($\delta = 0.4$ mm) and pipe wall thickness ($d = 16$ mm), but with different pipe diameters ($D_1 = 660$ mm, $D_2 = 762$ mm, $D_3 = 864$ mm, $D_4 = 1016$ mm); the same frost heave ($\delta = 0.4$ mm) and pipe diameter ($D = 813$ mm), but with different wall thickness ($d_1 = 10$ mm, $d_2 = 14$ mm, $d_3 = 18$ mm, $d_4 = 22$ mm). The pipe size parameters were selected based on the Pressure Piping Code (GB/T 20801.1–2020). The equivalent stress changes of pipes with different pipe diameters were calculated as shown in Figures 11 and 12.

The calculation results show that the pipe size has a significant effect on the equivalent stress of the pipe, especially on the stress peak at the interface. Figure 11 demonstrates that the larger the pipe diameter, the greater the equivalent stress. Under the condition of constant pipe diameter, the greater the oil pressure, the higher the temperature difference, the larger the foundation coefficient, and the greater the equivalent stress; raising the wall thickness can reduce the equivalent stress value. Under the same oil pressure (7 MPa), when the pipe diameter rises from 660 mm to 1016 mm, the equivalent stress increases from 356 MPa to 403 MPa, and the equivalent stress grows by 13.2% when the pipe diameter develops by 53.9% (Figure 11a). Under the same wall thickness (10 mm), the equivalent stress increases from 408 MPa to 465 MPa by 13.9% (Figure 11b). The equivalent stress increases by 13.7% from 341.2 MPa to 387.7 MPa for the same temperature variation (10 °C) (Figure 11c). Under the same foundation coefficient (25.8 MPa), the equivalent stress increases from 302 MPa to 342 MPa by 13.2% (Figure 11d). Overall, while other influencing factors remain constant, the pipe diameter increases by 53.9%, and the equivalent stress increases by about 13.5%. Figure 12 shows that appropriately increasing the wall thickness can effectively reduce the equivalent stress of the pipe caused by external factors when the external conditions are consistent. The greater the pipe wall thickness, the lower the oil pressure, the temperature difference, and the equivalent stress. Under the same oil pressure (7 MPa), the wall thickness increases from 10 mm to 22 mm, and the equivalent stress decreases from 434 MPa to 345 MPa by 20.5% when the pipe diameter increases by 53.9% (Figure 12a). The equivalent stress decreases by 15.6% from 379 MPa to 320 MPa under the same temperature difference (10 °C) (Figure 12b). It is worth noting that a higher oil pressure or a larger temperature difference will increase the equivalent stress, with the latter having a more significant effect. Therefore, under the condition of constant pipe diameter, altering the oil pressure in the pipe, the temperature difference inside and outside the pipe, the pipe wall thickness, or improving the properties of the foundation soil can enhance the deformation capacity of the pipe and alleviate the ultimate stress state of the pipe.

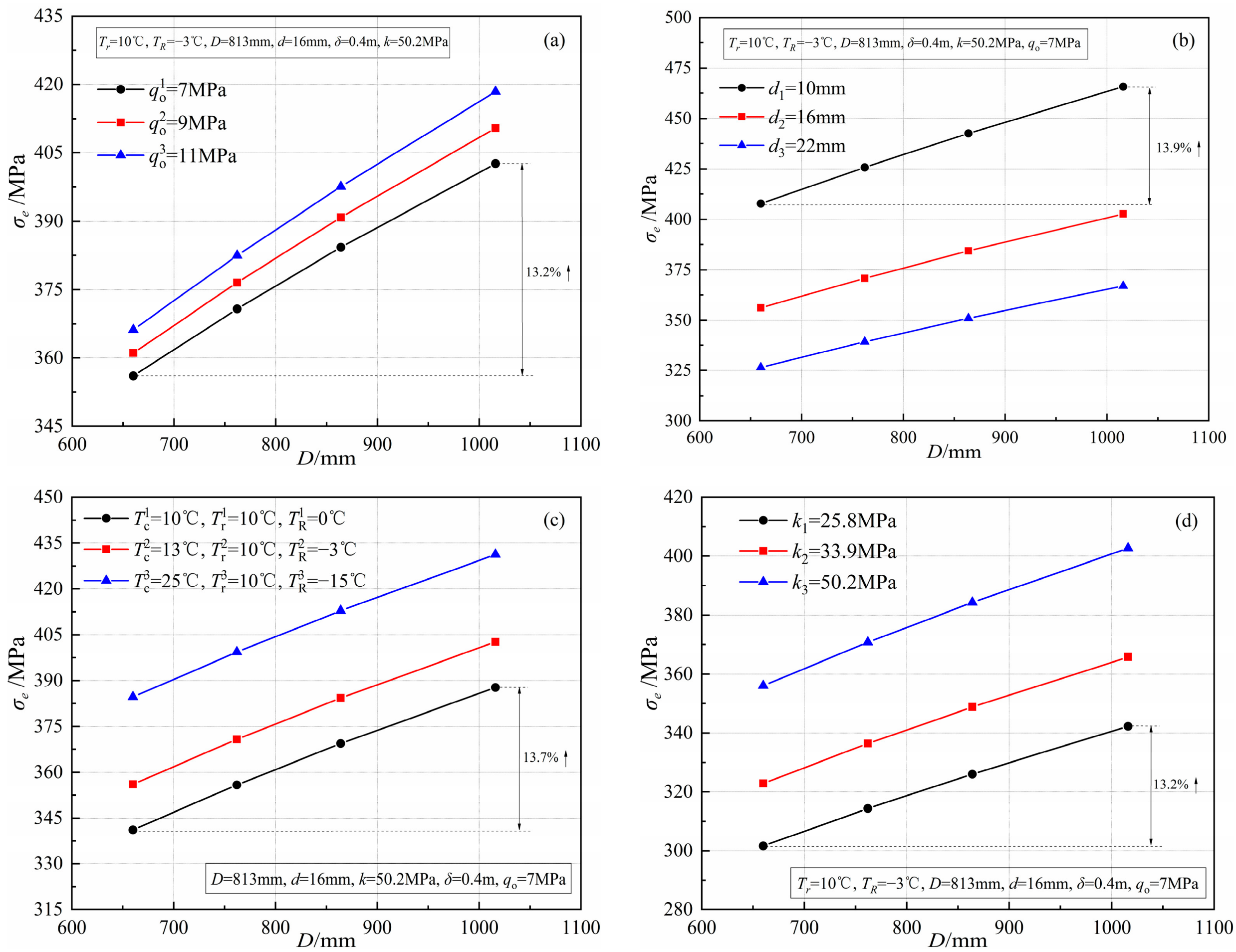

Figure 11. Variations in the equivalent stress with respect to the pipe diameter. (**a**) Under different oil pressures; (**b**) Under different wall thicknesses; (**c**) Under different temperature differences; (**d**) Under different foundation coefficients.

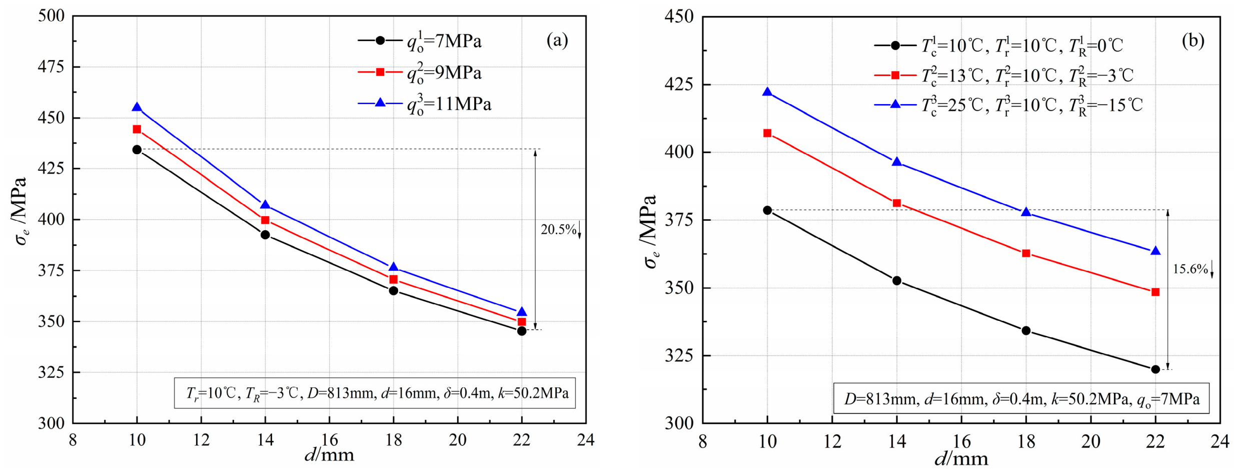

Figure 12. Variations in the equivalent stress with respect to the pipe wall thickness. (**a**) Under different oil pressures; (**b**) Under different temperature differences.

3.7. Elastic Modulus of Pipe (Material Properties)

Under the same pipe size (D = 813 mm, and d = 16 mm), the equivalent stress change law was analyzed with respect to the elastic modulus (E_p^1 = 180 GPa, E_p^2 = 195 GPa, E_p^3 = 200 GPa, and $E_p^4 = 206$ GPa) of the pipe changes, as shown in Figure 13 It can be seen that under the condition of constant pipe size when the pipe maintains the same frost heave deformation, the greater the pipe elastic modulus, the greater the pipe equivalent stress. Besides, the elastic modulus of the pipe increases linearly with the equivalent stress. The elastic modulus has a noticeable influence on the stress at the interface of different pipeline sections. Under the same oil pressure (7 MPa), the elastic modulus increases from 180 GPa to 206 GPa, the equivalent stress increases from 340.4 MPa to 373.9 MPa, the elastic modulus increases by 14.4%, while the equivalent stress increases by 9.8% (Figure 13a). Under the same temperature difference (10 °C), the equivalent stress increased from 305.1 MPa to 338.9 MPa, representing an increase of 11.1% (Figure 13b). Under the same foundation coefficient (25.8 MPa), the equivalent stress increased from 289.2 MPa to 317.1 MPa, representing an increase of 9.6% (Figure 13c). Under the same frost heave (0.4 m), the equivalent stress increased from 340.4 MPa to 373.9 MPa, representing an increase of 8.9% (Figure 13d). Overall, while keeping other influencing factors stable, the elastic modulus increases by 14.4%, and the equivalent stress increases by about 10%. In addition, if the pipe's elastic modulus is kept constant, the greater the oil pressure, the greater the temperature difference, the greater the foundation coefficient, and the greater the equivalent stress. This means that large oil pressure or temperature difference is an unfavorable factor for the stability of the pipeline.

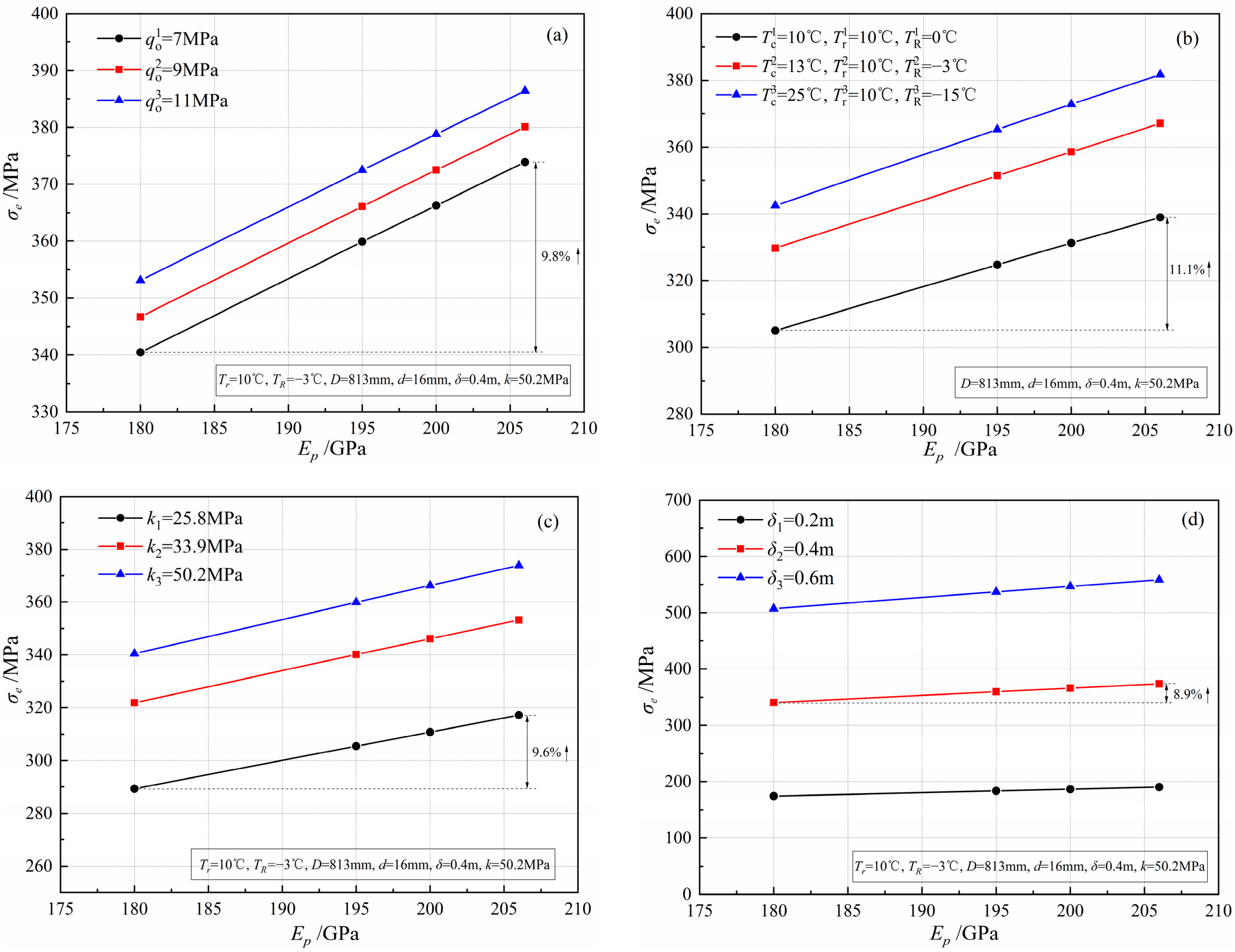

Figure 13. Variations in the equivalent stress with respect to the pipe's elasticity modulus. (**a**) Under different oil pressures; (**b**) under different temperature differences; (**c**) under different foundation coefficients; (**d**) under different frost heaves.

4. Discussion

Indeed, foundation frost heaving is a process of pipe–soil interaction with a complex stress characteristic that leads to pipeline bending deformation. Many factors affect the frost heaving of the foundation soil, including the soil's freezing characteristics, properties, moisture content, temperature, external load, and salt content. All external environmental factors affect and restrict each other. Hence, a quantitative analysis is required to explore relevant parameters' sensitivity and key indicators' change law during pipe–soil frost heaving. While this study attempts to provide some insights into the sensitivity of these influencing factors, the analysis discussed herein has certain limitations that need to be highlighted as follows:

(1) In pipelines with frost heaving damage, the complex terrain and geological conditions make the actual boundary conditions more complex. The pipe–soil interaction model and the stress form of the pipe are usually simplified in the calculation. The pipe stress, including internal and external forces, varies significantly under different environmental conditions, such as the pipe's self-weight, the weight and pressure of its fluid, the thermal expansion and cold contraction stress caused by temperature changes, the overlying soil weight, the traffic load, the ground surcharge, the additional forces caused by uneven settlement, and the seismic and frost-heaving forces. Considering all forces in the calculation is impossible. As a result, the main influencing factors should be considered in the design, or the secondary factors' influence coefficient should be reduced. Based on the dominant factors of the force, different stress conditions can be simplified into different calculation models [69]. However, the simplified model is undoubtedly different from the actual situation. For the analysis of longitudinal stress, the pipe is considered a whole flexible pipe; for the analysis of section stress, the pipe cross-section is considered an instantaneous rigid pipe. The pipe–soil model makes it difficult to estimate whether the pipe changes its section shape (ovalization) under non-uniform frost heaving pressure, which affects the pipe's circumferential stress and then leads to the increase of the equivalent stress of the pipe. In addition, there is stress concentration at the interface due to the derivative discontinuity at both ends of the transition region, which makes the calculated stress conservative and larger than the actual value and even exceeds the allowable stress of the pipe in some cases.

(2) The elastic modulus of a small amount of soil can be measured through laboratory tests, but it is not easy to come up with a definite value for the elastic modulus of a large soil amount. The elastic modulus is closely related to the soil's internal properties, such as temperature and water content, and it considerably affects the analysis of pipe–soil interaction. Frozen soil can be assumed elastic within a narrow strain range. Moreover, based on its mechanical properties, it has strong plasticity and viscosity (depending on its temperature, soil quality, and water content). Therefore, the elastic foundation beam theory approach underestimates the frozen soil's deformation capacity, thus the pipe's ability to withstand deformation.

(3) The overlying soil has an impact on the pipe's stress, the peak stress at the pipe top calculated according to the calculation method in Section 2.4 decreases linearly with the buried depth, and the change law is not significant; the soil pressure calculated by the above method does not consider the influence of soil freezing, which is not consistent with the actual situation. When the pipe top is covered with a thick soil layer, the downward frost-heaving force caused by the soil freezing is much larger than the soil pressure. In such a case, the above method significantly underestimates the pipe's restraint effect by freezing. On the other hand, when the soil layer in the seasonally frozen soil region encounters frost heaving, the freezing of the overlying soil layer extends downward from the ground surface and gradually forms a whole frozen body with greater stiffness. At this time, the resistance of the soil to the pipe deformation in the vertical direction also increases, and the downward freezing force can offset part of the upward bending stress of the pipe caused by frost heaving, which reduces the total stress at the pipe top. Therefore, thickening the overlying soil layer can reduce the stress caused by frost heaving and slow down the pipe deformation, mainly due to the downward frost action.

(4) In the elastic theory, under the same frost heave deformation condition, the lower the rigidity of the frozen soil, the more minor the damage to the pipeline by differential frost heave deformation. For the case of a short transition region, a small frost heave amount may cause great pipe stress, which is equivalent to the stress characteristics of the pipe when it encounters a frost mound, ice layers, and pingo. Therefore, when laying pipelines, it is necessary to avoid crossing those extreme geological terrain areas such as potential frost mounds, pingo, and high ice content areas. In addition, under a certain length of the frost-heaving region, the greater the differential frost heave deformation, the greater the pipe stress. However, the most unsafe place of the pipe is mainly at the interface of different sections. Therefore, the scope of the transition region is a critical element in pipeline design in seasonal frozen soil regions.

5. Conclusions

This paper comprehensively analyzes the relationship between the influencing factors and the mechanical parameters when the relevant parameters change by exploring various indices of pipe–soil interaction during frost heaving. Based on the physical parameters, materials, assumptions, and calculation methods given in this study, the following conclusions are drawn:

(1) Pipe stress changes considerably in the transition region between the non-frost heaving and the frost-heaving regions, with the peak stress occurring at the interface. The equivalent stress increases nonlinearly with the increase in the foundation coefficient. The greater the oil pressure in the pipe and the smaller the wall thickness, the greater the equivalent stress. The lower the temperature outside the pipe, the more significant the temperature difference and the greater the pipe peak stress.

(2) Frost heaving is the dominant factor of pipe stress and deformation, and the equivalent stress increases linearly with the change of frost heave. Considering the comprehensive influence of wall thickness and oil pressure, the smaller the wall thickness and the higher the oil pressure, the faster the maximum allowable frost heave deformation decreases.

(3) Under the same frost heave condition, the equivalent stress shows a nonlinear decreasing trend with the increase in the transition region length. The larger the frost heaving range, the more uniform the lifting effect on the pipeline and the smaller the influence on the pipe stress. The shorter the length of the transition region, the sharper the frost heaving, the steeper the displacement curve of the transition region, the greater the mutation at the interface, and the greater the stress peak.

(4) The pipe size significantly affects its equivalent stress, especially on the stress peak at the interface. The larger the pipe diameter, the greater the equivalent stress. The equivalent stress increases linearly with the elastic modulus, and increasing the wall thickness can effectively drop the pipe's equivalent stress due to frost heaving.

The relationship between various factors in the process of pipe–soil interaction is a complex problem. This paper has some limitations in reflecting the law of influencing factors by changing parameters. In the later stage, more accurate and reasonable constitutive relations of the pipe–soil system, a perfect pipe–soil model under frost heaving, and multi-field coupling calculation under multiple influencing factors are needed to reveal the interaction mechanism between the buried pipe and the frozen soil.

Author Contributions: L.H.: Methodology, Investigation, Writing—original draft, Formal analysis, Project administration, Funding acquisition; Y.S.: Conceptualization, Supervision, Resources, Writing—reviewing and editing; L.C.: Visualization, Writing—review and editing; E.P.: Validation, Software; X.H.: Software; X.Z.: Software, Data curation. All authors have read and agreed to the published version of the manuscript.

Funding: This research was funded by the "Qizhi" Talent Cultivation Project of Lanzhou Institute of Technology (Grant No. 2020QZ-04), the Fund for Young Doctor in Higher Education Institutions of Gansu Province (Grant No. 2021QB-127), and the Science and Technology Foundation for Youths of Gansu Province (Grant No. 22JR5RA386).

Institutional Review Board Statement: Not applicable.

Informed Consent Statement: Not applicable.

Data Availability Statement: Not applicable.

Acknowledgments: The authors would like to express their sincere thanks to funding organizations. The anonymous reviewers and editors provided valuable comments and suggestions for improving this manuscript.

Conflicts of Interest: The authors declare no conflict of interest.

References

1. Ma, Q.; Fu, H.; Xiao, H.; Xiao, H.; Liu, Y.; Zhang, J.; Deng, Q. Model test study on mechanical properties of pipe under the soil freeze-thaw condition. *Cold Reg. Sci. Technol.* **2020**, *174*, 103040. [CrossRef]
2. Mu, Q.; Wang, R.; Niu, Y.; Shi, Y.; Zhang, C. Mechanical analysis of a buried pipeline influenced by the soil frost heave and the axial force. *J. Lanzhou Univ. Nat. Sci.* **2021**, *57*, 278–284. [CrossRef]
3. Shen, M.; Ladanyi, B. Soil-pipe interaction during frost heaving around a buried chilled pipeline. In *Cold Regions Engineering*; ASCE: Reston, VA, USA, 1991; pp. 11–21.
4. Jin, H. Design and construction of a large-diameter crude oil pipeline in Northeastern China: A special issue on permafrost pipeline. *Cold Reg. Sci. Technol.* **2010**, *64*, 209–212. [CrossRef]
5. Li, G.; Cao, Y.; Ma, W.; Jin, X.; Chen, P.; Yu, Q.; Zhang, Z.; Mu, Y.; Jin, H. Permafrost engineering problem along China-Russia crude oil pipeline and mitigative measure. *Bull. Chin. Acad. Sci.* **2021**, *36*, 150–159. [CrossRef]
6. Chen, L.; Voss, C.I.; Fortier, D.; McKenzie, J.M. Surface energy balance of sub–Arctic roads with varying snow regimes and properties in permafrost regions. *Permafr. Periglac. Process.* **2021**, *32*, 681–701. [CrossRef]
7. Kim, K.; Zhou, W.; Huang, S.L. Frost heave predictions of buried chilled gas pipelines with the effect of permafrost. *Cold Reg. Sci. Technol.* **2008**, *53*, 382–396. [CrossRef]
8. Moser, A.P.; Folkman, S. *Buried Pipe Design*; McGraw-Hill Education: New York, NY, USA, 2008.
9. Xu, X.; Wang, J.; Zhang, L. *Physics of Frozen Soil*; Science Press: Beijing, China, 2010.
10. Huang, S.L.; Bray, M.T.; Akagawa, S.; Fukuda, M. Field investigation of soil heave by a large diameter chilled gas pipeline experiment, Fairbanks, Alaska. *J. Cold Reg. Eng.* **2004**, *18*, 2–34. [CrossRef]
11. Nixon, J.F.; MacInnes, K.L. Application of pipe temperature simulator for Norman Wells oil pipeline. *Can. Geotech. J.* **1996**, *33*, 140–149. [CrossRef]
12. Carlson, L.E.; Butterwick, D.E. Testing pipelining techniques in warm permafrost. In *Permafrost, Fourth International Conference, Proceedings*; National Academy Press: Washington, DC, USA, 1983; pp. 97–102.
13. Razaqpur, A.G.; Wang, D. Frost-induced deformations and stresses in pipelines. *Int. J. Pres. Ves. Pip.* **1996**, *69*, 105–118. [CrossRef]
14. Selvadurai, A.P.S.; Hu, J.; Konuk, I. Computational modelling of frost heave induced soil-pipeline interaction: II. Modelling of experiments at the Caen test facility. *Cold Reg. Sci. Technol.* **1999**, *29*, 229–257. [CrossRef]
15. Metje, N.; Chapman, D.N.; Walton, R.; Sadeghioon, A.M.; Ward, M. Real time condition monitoring of buried water pipes. *Tunn. Undergr. Space Technol.* **2012**, *28*, 315–320. [CrossRef]
16. Zheng, J.; Zhang, J.; Xu, J.; Liu, C.; Xu, L. Experiment on frost heave failure mechanism of PPR water pipe. *Eng. Fail. Anal.* **2020**, *117*, 104831. [CrossRef]
17. Calvetti, F.; Di Prisco, C.; Nova, R. Experimental and numerical analysis of soil–pipe interaction. *J. Geotech. Geoenviron. Eng.* **2004**, *130*, 1292–1299. [CrossRef]
18. Xu, G.; Qi, J.; Jin, H. Model test study on influence of freezing and thawing on the crude oil pipeline in cold regions. *Cold Reg. Sci. Technol.* **2010**, *64*, 262–270. [CrossRef]
19. Buco, J.; Emeriault, F.; Le Gauffre, P.; Kastner, R. Statistical and 3D numerical identification of pipe and bedding characteristics responsible for longitudinal behavior of buried pipe. In *Pipeline Division Specialty Conference*; ASCE: Chicago, IL, USA, 2006; pp. 1–10. [CrossRef]
20. Saberi, M.; Annan, C.; Sheil, B. An efficient numerical approach for simulating soil-pipe interaction behaviour under cyclic loading. *Comput. Geotech.* **2022**, *146*, 104666. [CrossRef]
21. Shao, Y.; Zhang, T. Elastoplastic pipe-soil interaction analyses of partially-supported jointed water mains. *J. Zhejiang Univ. Sci. A* **2008**, *9*, 1497–1506. [CrossRef]
22. Wu, Z.; Barosh, P.J.; Wang, L.; Hu, D.; Wang, W. Numerical modeling of stress and strain associated with the bending of an oil pipeline by a migrating pingo in the permafrost region of the northern Tibetan Plateau. *Eng. Geol.* **2008**, *96*, 62–77. [CrossRef]
23. Wen, Z.; Sheng, Y.; Jin, H.; Li, S.; Li, G.; Niu, Y. Thermal elasto-plastic computation model for a buried oil pipeline in frozen ground. *Cold Reg. Sci. Technol.* **2010**, *64*, 248–255. [CrossRef]
24. Wu, Y.; Sheng, Y.; Wang, Y.; Jin, H.; Chen, W. Stresses and deformations in a buried oil pipeline subject to differential frost heave in permafrost regions. *Cold Reg. Sci. Technol.* **2010**, *64*, 256–261. [CrossRef]
25. Su, W.; Wu, X. Numerical analysis and treatment of the frost heave deformation for buried gas pipelines. *Energy Res. Inf.* **2017**, *33*, 118–123. [CrossRef]

26. Vazouras, P.; Karamanos, S.; Dakoulas, P. Finite element analysis of buried steel pipelines under strike-slip fault displacements. *Soil Dyn. Earthq. Eng.* **2010**, *30*, 1361–1376. [CrossRef]
27. Rajeev, P.; Kodikara, J. Numerical analysis of an experimental pipe buried in swelling soil. *Comput. Geotech.* **2011**, *38*, 897–904. [CrossRef]
28. Tohidi, R.; Shakib, H. Response of steel buried pipelines to the three dimensional fault movement. *J. Sci. Technol.* **2003**, *14*, 1127–1135.
29. Trickey, S.A. Three Dimensional Finite Element Modeling of Buried Pipes Including Frost Action. Master Thesis, Queen's University, Kingston, ON, Canada, 2005.
30. Han, B.; Wang, Z.; Zhao, H.; Jing, H.; Wu, Z. Strain-based design for buried pipelines subjected to landslides. *Petrol. Sci.* **2012**, *9*, 236–241. [CrossRef]
31. Ogawa, Y.; Koike, T. Structural design of buried pipelines for severe earthquakes. *Soil Dyn. Earthq. Eng.* **2001**, *21*, 199–209. [CrossRef]
32. Akagawa, S.; Huang, S.L.; Kanie, S.; Fukuda, M. Movement due to heave and thaw settlement of a full-scale test chilled gas pipeline constructed in Fairbanks Alaska. In *OTC Arctic Technology Conference*; OnePetro: Richardson, TX, USA, 2012; pp. 1–11. [CrossRef]
33. Lin, Z.; Bai, X.; You, Y.; Wei, D. Sensitivity analysis of steel catenary riser TDZ under nonlinear pipe soil coupling. *Ocean Eng.* **2021**, *39*, 20–31. [CrossRef]
34. Chen, F.; Yu, J.; Zhao, Y.; Sun, Z.; Liu, J. Nonlinear buckling of subsea pipes with imperfection under complex loads. *J. Cent. South Univ.* **2015**, *46*, 2701–2706. [CrossRef]
35. Gao, F. Flow-pipe-soil coupling mechanisms and predictions for submarine pipeline instability. *J. Hydrodyn. Ser. B* **2017**, *29*, 763–773. [CrossRef]
36. Jiang, F.; Dong, S. Two-level quantitative risk analysis of submarine pipelines from dropped objects considering pipe–soil interaction. *Ocean Eng.* **2022**, *257*, 111620. [CrossRef]
37. Palmer, A.C.; Williams, P.J. Frost heave and pipeline upheaval buckling. *Can. Geotech. J.* **2003**, *40*, 1033–1038. [CrossRef]
38. Huang, C. Submarine Pipeline-Soil Coupling. Master Thesis, Harbin Engineering University, Harbin, China, 2011.
39. Karal, K. Lateral Stability of submarine pipelines. In *Offshore Technology Conference*; OnePetro: Richardson, TX, USA, 1977. [CrossRef]
40. Schotman, G.J.M.; Stork, F.G. Pipe-soil interaction: A model for laterally loaded pipelines in clay. In *Offshore Technology Conference*; OnePetro: Richardson, TX, USA, 1987. [CrossRef]
41. Hawlader, B.C.; Morgan, V.; Clark, J.I. Modelling of pipeline under differential frost heave considering post-peak reduction of uplift resistance in frozen soil. *Can. Geotech. J.* **2006**, *43*, 282–293. [CrossRef]
42. Li, G.; Ma, W.; Zhou, Z.; Jin, H.; Zhang, P. The limit state of pipeline based on strain design in cold regions. *J. Glaciol. Geocryol.* **2016**, *38*, 1099–1105. [CrossRef]
43. Huang, L.; Sheng, Y.; Wu, J.; Cao, W.; Peng, E.; Zhang, X. Experimental study on mechanical interaction between buried pipe and soil during freezing. *Cold Reg. Sci. Technol.* **2020**, *178*, 103129. [CrossRef]
44. Konrad, J.M.; Morgenstern, N.R. Frost heave prediction of chilled pipelines buried in unfrozen soils. *Can. Geotech. J.* **1984**, *21*, 100–115. [CrossRef]
45. Liang, J.; Gao, M.; Ba, Z. Stress analysis of municipal buried water pipes during cold wave period. *J. Saf. Environ.* **2019**, *19*, 436–443. [CrossRef]
46. Barber, J.R. *Intermediate Mechanics of Materials*; Springer: Dordrecht, The Netherlands, 2011; Volume 618.
47. Boresi, A.P.; Schmidt, R.J.; Sidebottom, O.M. *Advanced Mechanics of Materials*; Wiley: New York, NY, USA, 1985; Volume 6.
48. Huang, L.; Sheng, Y.; Hu, X.; Wang, S.; Huang, X.; He, B. Stress analysis of pipelines subjected to frost heave based on the theory of elastic foundation beam. *J. Glaciol. Geocryol.* **2018**, *40*, 70–78. [CrossRef]
49. Nixon, J.F.; Morgenstern, N.R.; Reesor, S.N. Frost heave–pipeline interaction using continuum mechanics. *Can. Geotech. J.* **1983**, *20*, 251–261. [CrossRef]
50. Foriero, A.; Ladanyi, B. Pipe uplift resistance in frozen soil and comparison with measurements. *J. Cold Reg. Eng.* **1994**, *8*, 93–111. [CrossRef]
51. Huang, Y.; He, F. *Beams, Plates and Shells on Elastic Foundation*; Science Press: Beijing, China, 2005.
52. Timoshenko, S.P.; Goodier, J.N. *Theory of Elasticity*; Xu, Z., Translator; Higher Education: Beijing, China, 2013.
53. Long, Y. *Calculation of the Beam on Elastic Foundation*; People's Education Press: Beijing, China, 1981.
54. Timoshenko, S.P. *Strength of Materials, Part II: Advanced Theory and Problems*, 3rd ed.; D. Van Nostrand Co., Inc.: New York, NY, USA, 1956; pp. 1–25.
55. Xu, Z. *Elastic Mechanics*; Higher Education: Beijing, China, 2006.
56. Thornton, D.E. Steady-state and quasi-static thermal results for bare and insulated pipes in permafrost. *Can. Geotech. J.* **1976**, *13*, 161–171. [CrossRef]
57. Zhang, Y. Numerical Simulation Study on Effects of the Buried Oil Pipeline on Permafrost Temperature. Master Thesis, Beijing Jiaotong University, Beijing, China, 2014.
58. Wang, F.; Li, G.; Ma, W. Progress in the research on the thermo-mechanical interaction between oil pipeline and permafrost in cold regions. *J. Glaciol. Geocryol.* **2022**, *44*, 217–228. [CrossRef]

59. Abduvayt, P.; Manabe, R.; Arihara, N. Effects of pressure and pipe diameter on gas-liquid two-phase flow behavior in pipelines. In *SPE Annual Technical Conference and Exhibition*; OnePetro: Richardson, TX, USA, 2003. [CrossRef]
60. Liu, Q. Calculating method and analysis of plane strain question of interaction between buried pipe and soil. *Rock Soil Mech.* **2007**, *28*, 83–88. [CrossRef]
61. Ainbinder, A.B.; Kamershtein, A.G. *Strength and Stability Calculation of Trunk Pipeline*; Xiao, Z.; Cui, D.; Qi, B., Translators; Petroleum Industry Press: Beijing, China, 1988.
62. Cheng, Z. Coupling of Temperature, Stress and Moisture Migration in Shallow Tunneling Using Multi-Freezing Pipes. Ph.D. Thesis, Central South University, Changsha, China, 2003.
63. Zhu, Y.; Zhang, J. Elastic and compressive deformation of frozen soils. *J. Glaciol. Geocryol.* **1982**, *4*, 29–40.
64. Tsytovich, N.A.; Swinzow, E.; Tschebotarioff, G. *The Mechanics of Frozen Ground*; Scripta Book Co: Washington, DC, USA, 1975.
65. Yao, B.; Liu, Z.; Wang, B.; Zhang, H. Experimental study of ultrasonic longitudinal wave measuring dynamic elastic modulus of frozen soil. *China Build. Mater. Sci. Technol.* **2009**, *18*, 85–88. [CrossRef]
66. Selvadurai, A.P.S. *Elastic Analysis of Soil Foundation Interaction*; Fan, W.; He, G.; Zhang, S.; Luo, W., Translators; China Railway Publishing House: Beijing, China, 1984.
67. Liu, Q. Soil-Structure Interaction Analysis of Buried Pipelines and Study of Its Stress & Deformation Calculating Method. Ph.D Thesis, Tongji University, Shanghai, China, 2002.
68. Li, G.; Wang, F.; Ma, W.; Fortier, R.; Mu, Y.; Zhou, Z.; Mao, Y.; Cai, Y. Field observations of cooling performance of thermosyphons on permafrost under the China-Russia Crude Oil Pipeline. *Appl. Therm. Eng.* **2018**, *141*, 688–696. [CrossRef]
69. Yang, J. Research on Longitudinal Mechanical Characteristics of Pipelines Buried in Soft Soil under Vertical Loads. Master Thesis, Zhejiang University, Hangzhou, China, 2006.